

INTERACTION OF CREEP, SHRINKAGE AND SHRINKAGE-INDUCED CRACKING OF CONCRETE

S. Reid and S. Sedra,
Department of Civil Engineering, University of Sydney,
Australia

Abstract

An extensive program of experimental testing and numerical modelling has been carried out to investigate the interrelated effects of shrinkage, shrinkage-induced cracking and creep of concrete. The shrinkage of concrete (including shrinkage-induced cracking) has been investigated using rectangular column specimens of three different sizes, and the creep of concrete has been investigated using tests on eccentrically loaded columns. Numerical modelling has also been carried out to investigate the behaviour of the shrinkage specimens, including the effects of shrinkage-induced cracking and the possible effects of the interaction between cracking and the diffusion of moisture from a drying specimen. Contrary to expectations (based on the anticipated effects of drying creep mechanisms), the creep test results have shown no consistent differences between the apparent compliance functions for axial and bending strain components of the loaded columns. Furthermore, the shrinkage test results have shown a size-effect which is not readily modelled using simple models of shrinkage-induced cracking and strain softening. The creep and shrinkage tests and the numerical modelling of shrinkage effects (including cracking) are summarised in the paper. Conclusions are presented concerning numerical modelling requirements to match the shrinkage test data.

Key words: Concrete, cracking, shrinkage, creep, tests, numerical models

1 Introduction

It is well-known that the deformation of concrete measured on a drying specimen loaded in compression exceeds the sum of the separate deformations associated with drying (of a non-loaded shrinkage specimen) and loading (of a sealed specimen) alone. The additional effect of simultaneous drying and loading is known as the Pickett effect (Pickett, 1942).

To account for the Pickett effect, concrete creep is commonly modelled in terms of a basic creep component (independent of drying) and an additive drying creep component. However, the mechanisms of drying creep are not fully understood, and there are significant uncertainties concerning the contributions of an 'apparent' drying creep mechanism related to shrinkage-induced stresses and associated cracking (Wittmann and Roelfstra, 1980), and a 'real' drying creep mechanism (Bazant and Xi, 1994). The deformation of drying concrete is further complicated by the interaction between shrinkage-induced cracking and the diffusion of moisture from a drying specimen.

An extensive program of experimental testing and numerical modelling has been carried out at the University of Sydney to investigate the interrelated effects of shrinkage, shrinkage-induced cracking and creep of concrete. The experimental work has been based on a novel series of tests on short concrete columns of rectangular section. The tests have been used to obtain measurements of surface strains for non-loaded specimens (drying shrinkage specimens and sealed specimens) and loaded specimens (drying and sealed), using specimens of 3 different sizes. The loaded column specimens have had eccentric compressive loads applied to produce strains associated with axial compression and bending about the major and minor principal axes of the section (with nominal compressive stresses over the entire cross section). Thus, for each loaded specimen, 3 correlated strain components (axial and biaxial bending components) have been measured, with each component affected differently by drying effects (i.e., drying creep and/or shrinkage-induced cracking). Accordingly, it was anticipated that differences between the apparent unit creep strain components would reflect differences in the relevant drying effects (noting that the effects of variations of relevant material properties and environmental conditions were eliminated, apart from variations within individual specimens).

Early test results (1987-90) appeared to show significant differences between axial creep and bending creep for drying specimens, and the observed differences were consistent with theoretical 'real' drying creep effects (Reid and Qin, 1990). Furthermore, corresponding tests on sealed specimens (1991) showed a convergence of the unit creep rates for the bending and axial strains, thereby supporting the tentative conclusion that the observed differences for drying specimens could be attributed to a real

drying creep mechanism. Accordingly, these results were reported and presented as evidence of a real drying creep mechanism (Reid, 1993).

However, later results from further extensive testing have shown no consistent relationship between the apparent unit creep strain components for bending and axial strains of loaded drying specimens. These later results are not consistent with a strong effect due to a real drying creep mechanism. Accordingly, the results are consistent with the hypothesis that the Pickett effect includes a significant contribution from an apparent drying creep mechanism involving shrinkage-induced cracking.

In order to investigate the effects of shrinkage and shrinkage-induced cracking, shrinkage strains have been measured on column specimens of 3 sizes, and extensive numerical modelling (involving non-linear diffusion, shrinkage, creep, strain-softening due to shrinkage-induced cracking, and coupling of diffusion and cracking) has been carried out to produce numerical results consistent with the shrinkage test results (including the effect of specimen size).

Details of the experimental test program and test results concerning shrinkage and drying creep are summarised below. Details and results of the relevant numerical modelling are summarised, and conclusions are presented concerning numerical modelling requirements to achieve consistency with the shrinkage test data.

2 Laboratory experiments

2.1 Design of experiments

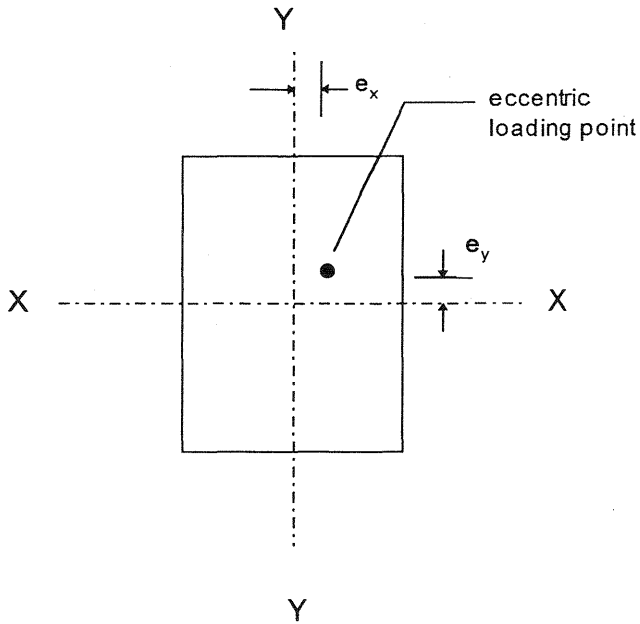
The experiments were designed to obtain measurements of (apparent) shrinkage strains and (apparent) creep strains of drying concrete specimens such that the measurements would characterise aspects of the interrelated effects of shrinkage, shrinkage-induced cracking and creep.

Shrinkage measurements were obtained from geometrically similar specimens of three different sizes: 75 x 50 x 250 (small); 150 x 100 x 500 (medium); and 300 x 200 x 1,000 (large).

The creep experiments were designed to obtain strain measurements for a comparison of creep in axial compression and creep in bending, whilst minimising the effects of cracking and variations of material properties and external environmental conditions. Accordingly, rectangular column specimens (medium and large, as above) were loaded eccentrically in compression to produce creep strains associated with axial compression and biaxial bending (as indicated in Figure 1). The section loading was designed to maximise the strains due to axial compression and bending, subject to constraints to ensure that: nominal stress distributions were similar for bending about the major and minor axes; nominal stresses due to the applied loading were compressive over the section; and the maximum

nominal compressive stress was approximately one quarter of the concrete strength.

Fig. 1. Eccentric loading



Several sets of creep measurements were obtained using medium and large specimens with various loads and load eccentricities as shown in Table 1.

Table 1. Creep test details

Set Number	Specimen Size	Load (kN)	Eccentricity	
			e_x (mm)	e_y (mm)
1	Medium	85	7.5	5.0
2	Medium	90	7.5	5.0
3	Medium	90	7.5	5.0
4a	Large	360	9.98	6.65
4b	Large	360	5.0	10.0

2.2 Preparation of test specimens

Each set of medium-sized creep test specimens was cast from a single batch of concrete with mix proportions (by weight) of: Type A Portland

cement, 19.4%; Basalt aggregate, 40.8%; Sydney sand, 29.5%; and tap water, 10.4%.

Each set of large creep test specimens (including companion shrinkage specimens) and each set of shrinkage test specimens was cast from commercial ready-mixed concrete with a specified 28-day cylinder strength of 40 MPa and a specified slump of 65 mm (without additives).

All specimens were cured in a fog room (at 22° C) until the commencement of testing.

2.3 Test equipment and instrumentation

The shrinkage and creep tests were all carried out in a control room maintained at 20° C and 50% Relative Humidity. The creep tests were carried out using spring-loaded creep frames, with loads transmitted to the specimens through the predetermined eccentric load points using ball bearings positioned in sockets in the end bearing plates (accurately cast in position in the specimen moulds).

Electronic strain gauges (and duplicate Demec gauges, in some cases) were positioned on the four faces of each specimen at mid-height.

2.4 Test results

2.4.1 Creep test results

Each set of creep test specimens contained four nominally identical specimens (cast from a single batch of concrete), including two specimens that were loaded (with nominally identical loads) and two companion (non-loaded) shrinkage specimens. Shrinkage strains were measured on the four faces of each shrinkage specimen, and the average shrinkage strains were determined. Total strains were measured on the four faces of each loaded specimen, and the total load-induced strains were estimated by subtracting the average shrinkage strains. The total load-induced strains of each loaded specimen were resolved into three components associated with axial compression and bending about the major and minor principal axes. The respective (average) compliance functions for the three strain components are shown in Figs 2-5 for creep test sets 1-4.

It was anticipated that the test results would show significant differences between the component compliance functions, consistent with the effects of a real drying creep effect (noting that the bending stiffness about the minor axis is the most sensitive to creep in the outer fibres where drying is greatest, and the axial stiffness is the least sensitive as it depends on creep and drying effects averaged over the cross-section). However, the differences between the component compliance functions shown in Figs 2-5 are dominated by apparently random effects.

It should be noted that the component compliance functions for bending were determined solely from the strains measured on the loaded specimens, whereas the compliance function for axial strains was determined from the

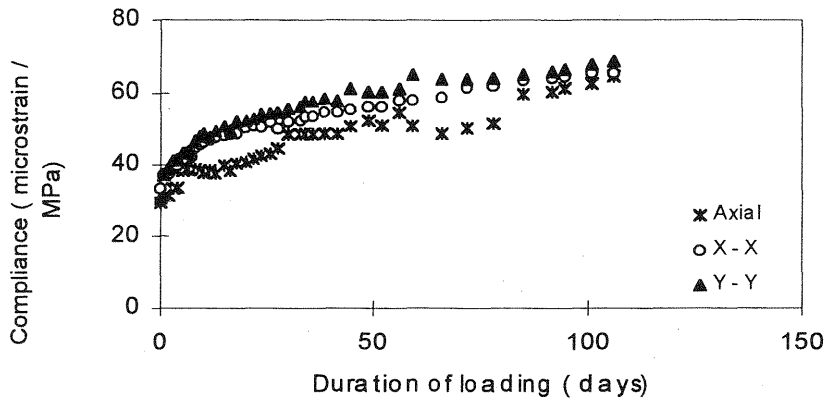


Fig. 2. Component compliance functions- Set 1

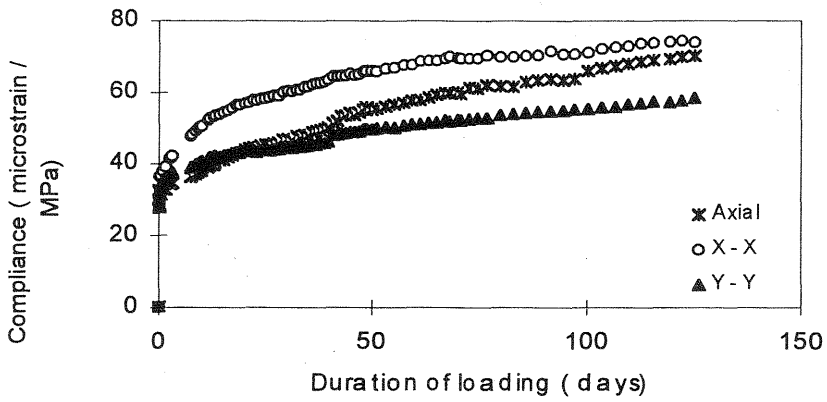


Fig. 3. Component compliance functions- Set 2

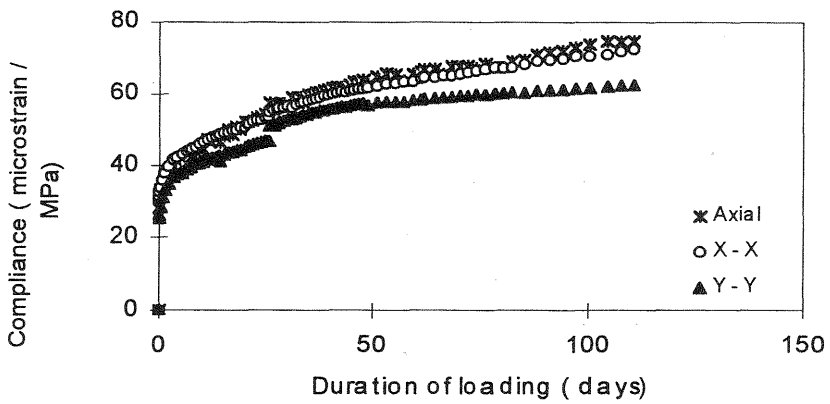


Fig. 4. Component compliance functions- Set 3

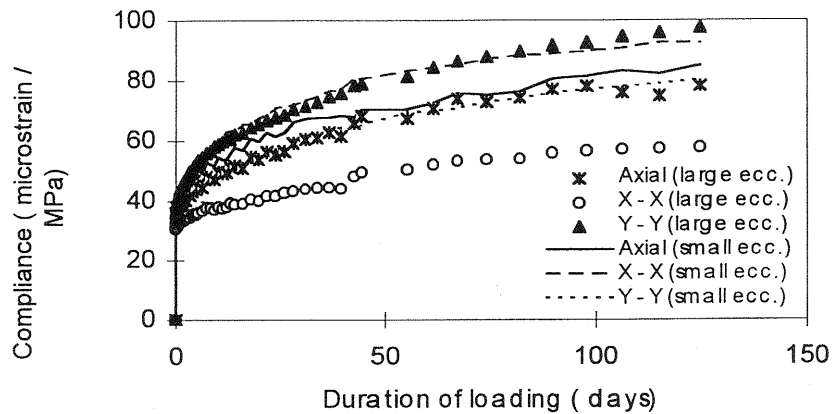


Fig. 5. Compliance component functions- Set 4a & Set 4b

difference between the strains measured on the loaded specimens and the strains measured on the companion shrinkage specimens. Accordingly the compliance for axial strains includes an extra contribution due to the effects of shrinkage-induced cracking in the non-loaded shrinkage specimens. It is therefore unexpected that the apparent compliance for axial strains is approximately the same as the compliance for the bending strains.

2.4.2 Shrinkage test results

Shrinkage measurements obtained from pairs of shrinkage specimens of three different sizes (prepared from the same batch of concrete) are shown in Figs 6-8. Each specimen size differs from the next size by a linear scale factor of 2, and the relevant size-effect is clearly evident in the results.

3 Numerical modelling

Numerical modelling of the shrinkage tests is described below.

3.1 Moisture diffusion

A nonlinear diffusion model (Bazant and Najjar, 1972) was used to model the diffusion of moisture for drying concrete. Values of the model parameters were chosen to fit the experimental results (giving $c_1=0.1$; $\alpha=0.05$; $h_c=0.9$; and $n=11$.)

3.2 Local shrinkage

Local (unrestrained) shrinkage at the elemental level was modelled assuming it was proportional to the change in relative humidity, with a coefficient of proportionality of 18 microstrain/(%RH).

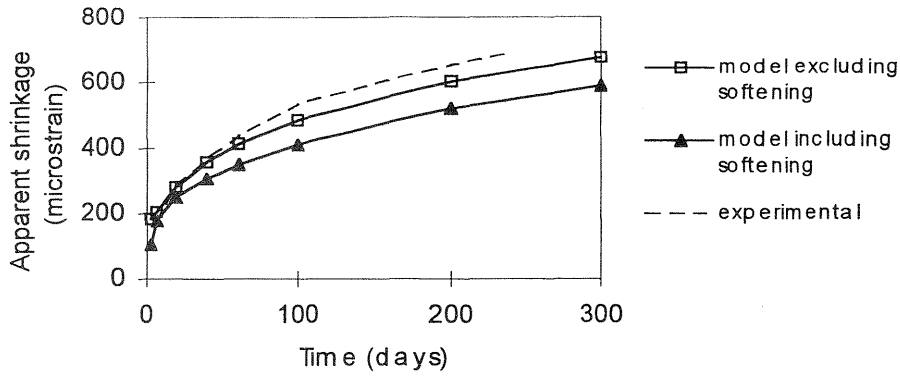


Fig. 6. Shrinkage for small specimen (75 x 50 x 250)

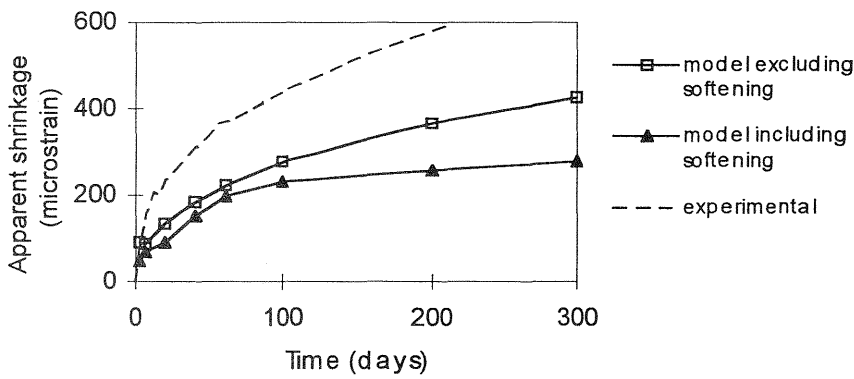


Fig. 7. Shrinkage for medium-sized specimen (150 x 100 x 500)

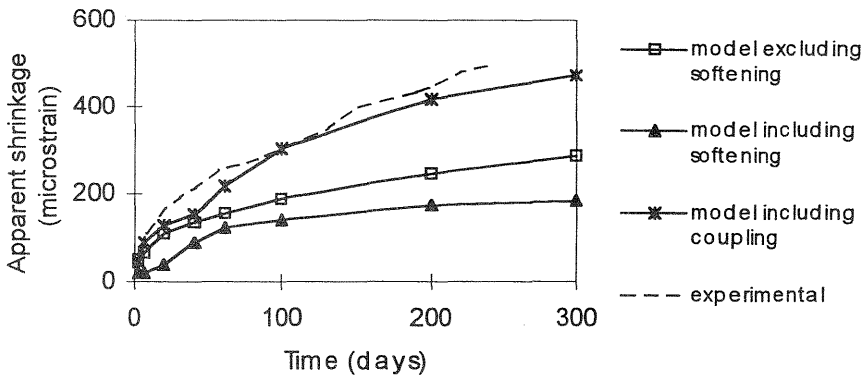


Fig. 8. Shrinkage for large specimen (300 x 200 x 1,000)

3.3 Stress and strain analyses

Finite element analyses of the stress and strain distributions were carried out with regard to time increments, using equivalent thermal stress analyses with equivalent temperature increments and time-dependent material properties including equivalent orthotropic expansion coefficients and orthotropic elastic (tangent) moduli to model the incremental strains and stresses developed in response to local shrinkage. The model of concrete compliance was based on the BP model (Bazant and Panula, 1980), but it excluded drying creep effects and it was expressed in terms of applied strain increments (to facilitate the modelling of strain-softening).

The numerical results based on the BP compliance model, excluding drying creep and ignoring strain-softening, are shown in Figs 6-8, together with the experimental results. It can be seen that the numerical results show reasonable agreement with the experimental results for the small specimens. However, the numerical model significantly under-estimates the shrinkage strains for the larger specimens, and the degree of under-estimation increases with the specimen size.

The effects of strain-softening due to shrinkage-induced cracking were also modelled. Strain-softening was modelled as an effectively elasto-plastic response, with a negligible tangent modulus for tensile strain increments when the cumulative 'elastic' tensile strain exceeded 0.00005 (corresponding to a tensile strength of 3.15 MPa). The numerical results including strain-softening due to shrinkage-induced cracking are also shown in Figs 6-8. Clearly strain-softening reduces the apparent shrinkage strains, consistent with an apparent drying-creep effect. However, the effect of strain-softening is greater for the larger specimens than the small specimens. Thus the strain-softening model exacerbates the relative under-estimation of shrinkage strains for the larger specimens.

However, shrinkage-induced cracking would cause not only strain-softening but also accelerated diffusion of moisture from the drying concrete. Accelerated diffusion would counteract the reduction in apparent shrinkage due to strain-softening. In order to model the possible effects of accelerated diffusion, it was assumed that the diffusion through a cracked element increased in proportion to the 'post-cracking' strain (up to a factor of 100 at a post-cracking strain of 0.001). To model the effect of cracking on the diffusion of moisture through the concrete, it was necessary to couple the diffusion and stress/strain (strain-softening) analyses. The results of the coupled analyses for the large specimen are shown in Fig. 8. The results of the coupled diffusion and strain-softening analyses show that the increase in shrinkage due to accelerated diffusion could be greater than the decrease in shrinkage due to strain-softening. Accordingly, it would be possible to model the observed shrinkage size-effect using a coupled diffusion model, but that would not be consistent with the strain-softening explanation for an apparent drying creep mechanism.

4 Conclusions

The Pickett effect is generally attributed to a real drying creep mechanism and shrinkage-induced cracking in drying concrete (producing apparent drying creep effects). Creep strains of eccentrically loaded columns have shown no strong effects attributable to real drying creep. On the other hand, numerical modelling has shown that strain-softening due to shrinkage-induced cracking could significantly reduce apparent shrinkage strains and produce strong apparent drying creep effects. However, it has also been shown that such strain-softening effects are not consistent with an observed size-effect for shrinkage strains of geometrically similar specimens. The observed shrinkage size-effect could be modelled using a combination of strain-softening and accelerated moisture diffusion for cracked concrete, but then shrinkage-induced cracking would not give an apparent drying-creep effect. The Pickett effect needs further explanation.

5 References

- Bazant, Z.P., and Najjir, L. (1972) Nonlinear water diffusion in nonsaturated concrete. **Mater. & Struct.**, 5, 3-20.
- Bazant, Z.P., and Panula, L. (1980) Creep and shrinkage characterisation for analysing prestressed concrete structures. **J. PCI**, 25, 86-122
- Bazant, Z.P., and Xi, Y. (1994) Drying creep of concrete: constitutive model and new experiments separating its mechanisms. **Mater. & Struct.**, 27, 3-14.
- Pickett, G. (1942) The effect of change in moisture content on the creep of concrete under a sustained load. **J. ACI**, 38, 333-355.
- Reid, S.G., and Qin, Q.C. (1990) Comparison of concrete creep strains due to bending and axial compression. **NSEC2**, IEAust, Adelaide, 255-258.
- Reid, S.G. (1993a) Deformation of concrete due to drying creep, in **Creep and Shrinkage of Concrete** (eds Z.P. Bazant and I. Carol), E.& F.N. Spon, London, 39-44.
- Reid, S.G. (1993b) A new approach to drying creep of concrete. **ACMSM** 13, Wollongong, Australia, 721-728.
- Wittmann, F.H., and Roelfstra, P. (1980) Total deformation of loaded drying concrete. **Cem. & Concr. Res.**, 10, 601-610.